processes

MDPI

Article

A Quantitative Examination of the Efficiency of a Biogas-Based Cooling System in Rural Regions

Kenan Saka

Department of Machinery, Yenişehir İbrahim Orhan of Vocational School, Bursa Uludağ University, 16900 Bursa, Türkiye; kenansaka@uludag.edu.tr

Abstract: This study investigates the efficiency of a biogas-powered cooling system through the utilization of energy and exergy calculations. Biogas, which can be generated and stored in small-scale plants as needed, serves as a viable fuel source for absorption cooling systems. The present research focuses on the biogas consumption of a triple-effect absorption cooling system specifically designed to supply a fixed cooling load of 100 kW under varying operational conditions. This study highlights the coefficient of performance and exergetic coefficient of performance values of the system, along with the exergy destruction rates of its individual components, at the optimal temperatures of operation. Furthermore, to determine necessary biogas consumption, this study explores the establishment of dedicated farms for various animal species, ensuring an adequate number of animals for biogas production. The findings reveal a coefficient of performance of 1.78 and an exergetic coefficient of performance of 35.4% at the optimized operating temperatures. The minimum mass flow rate of biogas is determined to be 0.0034 kgs^{-1}, facilitating the operation of the boiler with a methane content of 65%. This study concludes that a total of 290 head of cattle is required to generate the annual biogas consumption necessary for the cooling system. Additionally, the number of the cattle is enough to establish 284 biogas plants in Bursa Province in Türkiye.

Keywords: biogas-powered cooling system; energy and exergy analysis; triple-effect absorption cooling system; animal species; methane content

Citation: Saka, K. A Quantitative Examination of the Efficiency of a Biogas-Based Cooling System in Rural Regions. *Processes* **2023**, *11*, 1983. https://doi.org/10.3390/pr11071983

Academic Editors: Kai Yan, Ahmed Elwardany and Mahmoud Omar Amer

Received: 18 May 2023
Revised: 21 June 2023
Accepted: 27 June 2023
Published: 30 June 2023

1. Introduction

Most cooling systems rely on electricity, but absorption chillers offer alternative approaches to a sustainable energy future. Absorption cooling systems can utilize the thermal power derived from industrial waste heat sources as a driving force along with renewable energy sources such as biogas. The available options in the market include single-effect, double-effect, and triple-effect systems. Higher-effect cycles aim to enhance system performance, particularly when a high-temperature heat source is available [1]. The performance of these systems is typically evaluated using the coefficient of performance (COP) or exergetic coefficient of performance (ECOP).

The literature extensively elucidates the operation and arrangement of absorption cycles [1–4]. Among these, the single-effect cycle represents the most straightforward configuration. Utilizing the single-effect cycle as a foundation, more intricate cycles can be devised to enhance either energy efficiency or the attainable temperature difference between the evaporator and generator. The double- and triple-effect cycles achieve higher COPs compared to the single-effect cycle, albeit necessitating an energy input at elevated temperatures. While each system features a single evaporator and absorber, the double- and triple-effect cycles employ a greater number of condensers and generators. The design of absorption cooling systems differs from that of traditional systems, as it eliminates the need for an electrical compressor, resulting in a more complex thermodynamic calculation. Saka [2] demonstrated that increasing the low-pressure generator (LPG) and evaporator temperatures while lowering the condenser temperature can improve the COP. Azhar

and Siddiqui [3] conducted a thermodynamic analysis of triple-effect vapor absorption cooling cycles using H_2O-LiBr as the working fluid. They explored the use of liquefied petroleum gas and compressed natural gas as energy sources. The researchers calculated the maximum COP of the triple-effect cycle to be 1.955, with a fixed evaporator cooling capacity of 300 kW. In another study, the same researchers focused on the exergy analysis and optimization of the operating conditions for single- to triple-effect absorption cycles. They found that the triple-effect cycle outperformed the single- and double-effect systems in terms of the ECOP and COP, making it more economically viable and efficient [4].

Absorption systems can be integrated into more advanced setups. Mahmodi and Yari [5] integrated a triple-effect absorption system with a water desalination system to produce distilled water. For subzero temperature applications, H_2O-LiBr is not a suitable working fluid. Gkouletsos et al. [6] investigated the use of NH_3-H_2O as the working fluid for triple-effect absorption refrigeration processes. They explored multiple thermodynamic models and observed close agreement with the literature values for single-effect and double-effect systems, with slight deviations for the triple-effect system.

Ruwa et al. [7] proposed a biogas-powered multigeneration system with a single-effect absorption chiller. They performed energetic and exergetic analyses, considering three types of biogas. The study aimed to provide insights for future practical designs for electricity production from waste and biomass materials. Velazquez et al. [8] analyzed a geothermal field in Mexico to compare the performance of absorption cooling systems driven by geothermal sources. They found that an advanced triple-effect system could potentially provide a cooling potential of 92.995 GW. Lizarte and Marcos [9] optimized the COP of a triple-effect parallel-flow H_2O-LiBr absorption chiller under both design and off-design conditions. They emphasized that the current market configuration of absorption chillers predominantly uses series flow. Their results are relevant for optimizing the control regulations in future parallel-flow prototypes driven by variable temperature sources, such as solar energy. Gebreslassie et al. [10] reported the maximum COP of a series-flow triple-effect absorption cooling system to be 2.312 and the maximum COP of a parallel-flow triple-effect system to be 2.321. They also determined the exergetic efficiency of the series-flow system to be 44.7% and that of the parallel-flow system to be 47%.

Absorption cooling systems can be cascaded with vapor compression systems. Agarwal et al. [11] presented a theoretical analysis of an absorption–compression cascade refrigeration cycle. They coupled a triple-effect series-flow H_2O-LiBr absorption cooling cycle with a vapor compression refrigeration cycle using refrigerant R1234yf through a cascade heat exchanger. Schneider et al. [12] conducted a study on a trigeneration system, specifically a small-scale biogas-based plant. This system was primarily designed to meet the low cooling demands required for milk preservation in small dairy farms. The study presented various scenarios, and the results demonstrated superior energy performances compared to the reference fossil-fuel-based energy solutions, resulting in savings of up to 31% in primary energy utilization.

In a separate study, Bamisile et al. [13] developed and analyzed a novel trigeneration system that operates on biogas generated from chicken manure and maize silage. The objective of the performance analysis was to achieve higher efficiencies in the system. The overall energy and exergy efficiency of the developed trigeneration system were reported to be 64% and 34.51%, respectively. The highest exergy destruction within the system was observed in the combustion chamber. Sevinchan et al. [14] conducted energy and exergy analyses on a biogas-driven multigenerational system which encompassed various subsystems, including a biomass digester, Brayton cycle, organic Rankine cycle (ORC), single-effect absorption chiller, heat recovery unit, and water separation unit. The study revealed that the multigenerational system achieved a maximum exergy efficiency of 30.44%, with the combustion chamber accounting for 65% of the highest exergy destruction rate.

Anand et al. [15] performed a numerical study to critically analyze a biogas-powered absorption system for climate change mitigation. The system under investigation was

a biogas-powered NH_3-H_2O absorption refrigeration system, where biogas was utilized to heat the water, serving as an energy input to the generator of the absorption system. The results indicated that the generator experienced the highest exergy loss, while the condenser exhibited the lowest exergy loss. Maryami and Dehghan [16] conducted an exergetic evaluation of thermodynamic flows at a cooling capacity of 300 kW. The study involved a comparison of five different absorption systems operating with H_2O-LiBr, and the optimum generator temperature was determined based on the maximum efficiencies. The results showed that the triple-effect cycle exhibited variation ranges of the maximum COP and exergetic efficiency of 1.482–1.905 and 14.21–24.09%, respectively.

Hot water, steam, and hot air are widely used as heat sources in absorption applications. Kaynakli et al. [17] suggest that a cooling system can be driven by these heat sources through a high-pressure generator (HPG). The authors conducted an energy and exergy analysis on a double-effect series flow absorption cooling system using H_2O-LiBr as the working fluid pair. Their findings indicate that the exergy destruction of the HPG increases as the temperature of the heat sources rises. Specifically, the destruction is maximized when hot air is utilized as the heat source, while it is minimized when hot water is used.

Yılmaz et al. [18] investigated the internal thermal balance of a double-effect absorption cycle. They demonstrated that properly designating the high-pressure condenser temperature enhances the COP and ECOP due to its significant impact. The designated temperature should necessarily be higher than the outlet temperature of the LPG. Additionally, Yılmaz et al. [19] examined the effects of critical operational constraints, such as the concentration equivalence state, the thermal imbalance between system components, and the risk of freezing and crystallization, on the operational range and performance of a double-effect H_2O-LiBr absorption refrigeration system. The authors reported that the proposed system can improve the COP by up to 31% and the ECOP by up to 84%.

Caetano et al. [20] highlighted the potential of biogas as an alternative energy source for regions distant from conventional power production and distribution centers. To demonstrate this alternative, they evaluated a decentralized biogas production system and its utilization for power generation through external combustion engines. The authors examined the life cycle of biogas on a rural property and investigated the number of animals required for energy production in livestock farming in rural areas. In their study, the biogas produced in the biogas digester was directed to a burner, and the heat generated by combustion was used as an energy source for the engine. They reported that, considering an average methane content of 60% among the tested values, 13 dairy cows are required for the continuous generation of 1 kWh.

Yılmaz and Saka [21] conducted an assessment to determine the potential of the exploitable agricultural biomass in the Southeastern Anatolia Region of Türkiye based on the regional data released by the Ministry of Energy and Natural Resources. The study considered both animal- and vegetal-derived biomasses. A total of 16 animal species and 94 vegetable species found in the region were taken into account. The animal species comprised five poultry species, two small ruminant species, and eight cattle species. The study considered the energy utilization of animal manure through anaerobic digestion for manure treatment, resulting in the production of biogas, which is a mixture of methane and carbon dioxide. The methane content in the biogas ranged between 55% and 75%. The findings indicate that the Southeastern Anatolia Region has the potential to contribute 8.2% to the country's total biomass energy yield.

A commercial firm has recently announced itself as the first manufacturer of triple-effect absorption chillers. The company has achieved a significant breakthrough in the air-conditioning field by commercializing this advanced absorption technology. According to the company, triple-effect absorption chillers have a COP of 1.8, which is nearly 30% higher than that of double-effect absorption chillers. This advancement enables users to significantly reduce their energy requirements for cooling [22].

Considering the aforementioned factors, this study makes novel contributions to the following aspects. Firstly, it investigates the impact of critical operational constraints on

the operational domain and performance of a triple-effect series-flow H_2O-LiBr absorption cooling system. These constraints encompass the equivalence state of concentrations, the thermal imbalances between internal condensers and generators, and the risk of freezing and crystallization of the H_2O-LiBr solution. A simulation program with a detailed solution procedure was developed for system analysis, enabling energy and exergy analyses. This study demonstrates the system's COP, ECOP, and exergy destruction at the optimal component temperatures. Secondly, the investigated system is powered by an indirect fired biogas boiler. The composition of biogas can vary, with the methane content ranging from 80% to 40%. Consequently, the lower heating value (LHV) of biogas exhibits variations based on the percentage of methane and carbon dioxide that is present. This study presents the mass flow variations of biogas for five different methane contents, emphasizing the minimum biogas consumption value. Thirdly, this study explores the establishment of specialized farms for each species, aiming to determine the sufficient number of animals needed for sixteen different species to generate the required biogas consumption for powering a 100 kW cooling capacity. Additionally, the number of biogas power plants that can be established according to the biomass potential is given for Bursa Province, located in Türkiye. This study does add value to the literature, as this novel case study has never been done for this specific location and climate.

2. Materials and Methods

2.1. System Description

Figure 1 illustrates a standard farm equipped with a biogas plant and an absorption cooling system. The biogas plant employs a biodigester system to convert biomass into a combustible fuel source. Subsequently, this biogas can be utilized as an alternative fuel in a steam boiler system, where it undergoes digestion to produce steam. The generated steam serves as the necessary energy input for the absorption cooling system.

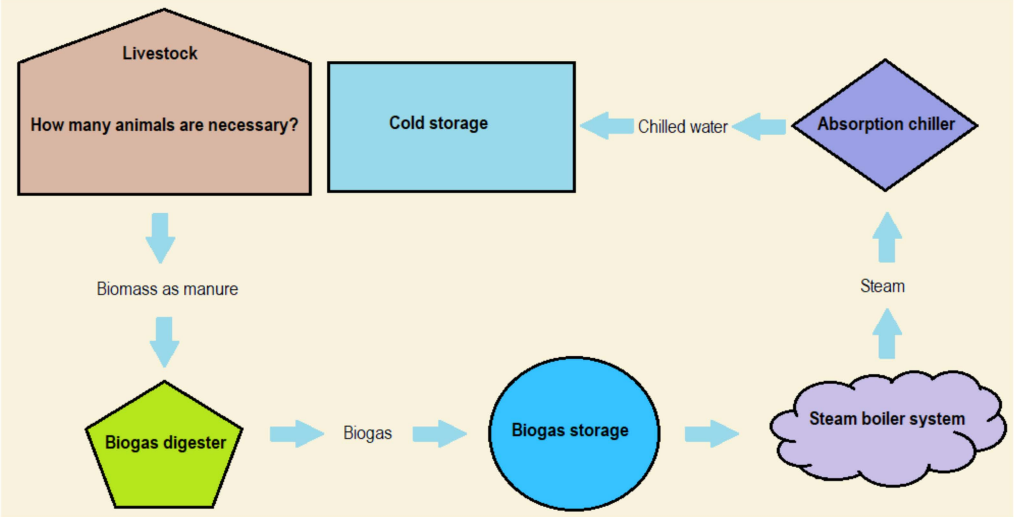

Figure 1. Energy generation during livestock production in rural area.

The absorption chiller utilizes steam to drive the lithium bromide cooling cycle, enabling the production of chilled water. Since the absorption chiller relies on heat for the cooling process, it consumes only a minimal amount of electricity to operate the unit's pumps. The chilled water produced by the absorption system is then utilized for cold storage purposes. Examining the entire system, the energy flow originates from the livestock section of the farm. The number of animals present determines the required energy source to achieve the desired cooling capacity.

Figure 2 presents a comprehensive depiction of the intricate components and parts comprising a triple-effect absorption cooling system. In contrast to traditional electrical

compressors, a triple-effect absorption cooling system employs absorbers and generators to achieve cooling. A key component of the system is the HPG, which facilitates the utilization of diverse energy sources. In this particular configuration, a biogas boiler functions as a heat source to generate steam. The system also incorporates a medium-pressure generator (MPG) and an LPG as internal components.

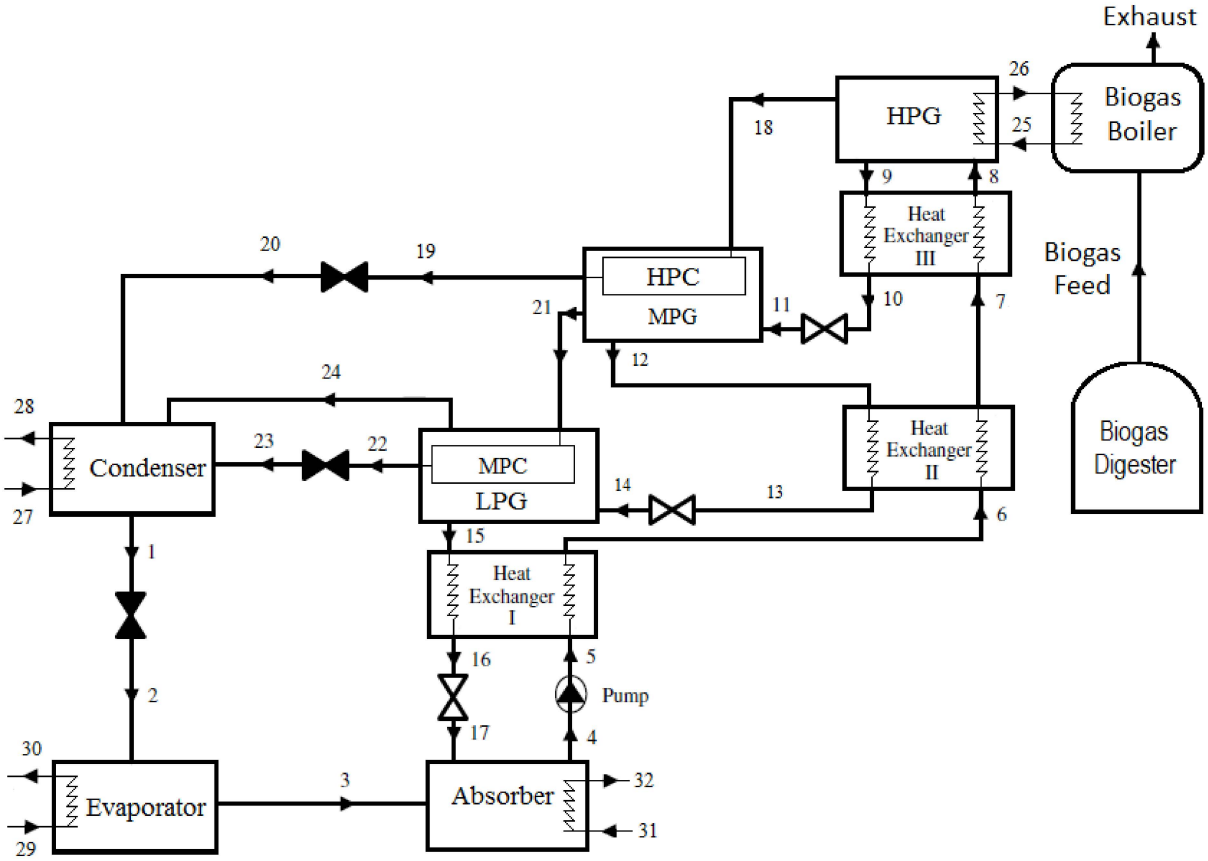

Figure 2. Triple-effect series-flow absorption cooling system flowchart [2].

During operation, the superheated vapor produced by the HPG (point 18), MPG (point 21), and LPG (point 24) is condensed by the high-pressure condenser (HPC) (points 19–20), medium-pressure condenser (MPC) (points 22–23), and condenser (points 1–2), respectively. The remaining vapor is subsequently transferred to the condenser. Other essential elements of the system include the evaporator, expansion valves, solution pump, and solution heat exchangers (SHEs).

The system encompasses four distinct pressure and concentration levels, which contribute to its complexity throughout the cycle. The flow rates within the system components and parts are directly related to heat transfer interactions with the environment.

Concentration level I (points 4–8)

Concentration level II (points 9–11)

Concentration level III (points 12–14)

Concentration level IV (points 15–17)

The HPG, evaporator, and pump play crucial roles in providing energy input to the system. The evaporator (point 3) extracts heat from the cold storage volume (points 29–30) to generate the desired cooling effect. The term "heat exchanger" encompasses any system component involved in heat transfer; however, internal heat exchangers have been distinctively segregated from condensers or generators. Additionally, the inclusion of internal heat exchangers serves to diminish the thermal capacity of the HPG, consequently bolstering the overall performance of the system. The system in question comprises three internal SHEs. The effectiveness of a heat exchanger is defined as the ratio between the actual heat

transfer and the maximum achievable heat transfer. Consequently, the effectiveness of heat exchangers I, II, and III is denoted by the symbol ε.

The thermodynamic analysis of the aforementioned absorption system is conducted through theoretical means, employing principles of mass and energy balance. These fundamental equations are applied to the various components and parts of the system operating under steady-state conditions.

The equations involved in the analysis encompass numerous parameters. In order to solve the complete set of model equations, estimation of the thermal balance temperature within the HPC and MPG, as well as the MPC and LPG units, is necessary. In this study, a more realistic approach was adopted by considering the inequality of outlet temperatures, as it offers greater physical insight into the system's behavior. To facilitate this approach, a dedicated computer program was developed, employing a solution algorithm to predict the unknown variables.

2.2. Thermodynamic Analysis

To facilitate the thermodynamic analysis of the system, the mass and energy conservation equations were incorporated into the simulation program to determine the component loads. The general forms of these balance equations are provided below [1]. The preservation of mass within the system was ensured through the utilization of the mass balance equation, which takes into account the inflows and outflows of mass in each system component. On the other hand, the conservation of energy within the system was guaranteed by the energy balance equation, which considers the transfers of energy in the form of heat, work, and other relevant energy forms for each component. These fundamental balance equations served as the cornerstone for computing the diverse thermodynamic properties and performance parameters of the system throughout the simulation process. Mass inlet and exit:

$$\sum \dot{m}_i = \sum \dot{m}_e \tag{1}$$

Concentration balance:

$$\dot{m}_i X_i = \dot{m}_e X_e \tag{2}$$

Energy inlet and exit:

$$\left(\sum \dot{m}_i h_i - \sum \dot{m}_e h_e\right) + \left(\sum Q_i - \sum Q_e\right) + W = 0 \tag{3}$$

The effectiveness of heat exchangers I, II, and III are respectively given as follows:

$$\varepsilon = \frac{h_i - h_e}{h_i - h_e^*} \tag{4}$$

where h^*_e represents the enthalpy of minimum heat capacity streams (here, it is hot stream, i.e., strong solution) at the exit of the respective heat exchangers when they are cooled to the temperature of respective entry cold streams (weak solution).

The overall energetic performance of the plant is determined by evaluating its COP:

$$\mathrm{COP} = \frac{\dot{Q}_E}{\dot{Q}_{HPG} + \dot{W}_P} \tag{5}$$

The initial stage in analyzing the efficiency of the triple-effect absorption cooling system involved applying the first law of thermodynamics. Subsequently, second-law analysis was employed to evaluate the system's performance based on exergy, which inherently diminished due to thermodynamic irreversibilities. Exergy can be broadly defined as the maximum potential work that a substance or energy form possesses relative

to its surroundings. The analysis of exergy destruction aimed to determine the extent of exergy loss and inefficiency within the system. It is formulated as,

$$\psi = (h - h_0) - T_0(s - s_0) \tag{6}$$

The exergetic efficiency can be calculated as follows (ECOP):

$$\text{ECOP} = \frac{-\dot{Q}_E(1 - T_0/T_E)}{\dot{Q}_{HPG}(1 - T_0/T_{HPG}) + \dot{W}_P} \tag{7}$$

where i is inlet, e is exit, $\dot{m}$ is mass flowrate in kgs^{-1}, X is solution concentration in %, h is enthalpy in kJ/kg, s is entropy in kJ/kg-K, $\dot{Q}$ is heat transfer rate in kW, $\dot{W}$ is work rate in kW, E is evaporator, and T_0 is reference temperature.

Table 1 presents the capacities of the components, namely HPG, condenser, and absorber, within the triple-effect absorption cooling system under a specified cooling load. A numerical comparison with relevant literature is also provided. The literature has previously demonstrated the validity of the algorithm used to calculate energy and exergy based on the associated equations [17–19]. The absorber exhibited the highest load among the components, while the pump exhibited the lowest load. To ensure practical convenience, a cooling capacity, i.e., $\dot{Q}_E$, of 100 kW [15] was chosen as a reference to proportionally assign heat capacities to the remaining system components. Fixed cooling capacity approach is commonly accepted in the literature;

- 1000 kW [10];
- 500 kW [5];
- 300 kW [1–4];
- 1 kW [9].

Table 1. Comparison of calculated component capacities.

T_{HPG} = 190 °C, $\varepsilon_{I,II,III}$ = 0.85, T_A = 33 °C, T_E = 4°C, T_C = 33 °C		
Components	**Load (kW) Present Study**	**Load (kW) Gomri [23]**
HPG, $\dot{Q}_{HPG}$	170.40	169.68
Condenser, $\dot{Q}_C$	115.32	112.23
Evaporator, $\dot{Q}_E$	300.00	300.00
Absorber, $\dot{Q}_A$	355.39	357.67
Pump, $\dot{W}_P$	0.23	0.22
COP	1.76	1.76

2.3. Assumptions

In the analyses, certain assumptions were made to simplify the solution process [24]. The system was operated under standard reference conditions, with an ambient temperature of 25 °C and atmospheric pressure of 1 atm. Pressure losses in heat exchangers and pipelines were assumed to be negligible. It was assumed that the water at the outlet of the condenser existed in a saturated liquid state, while at the outlet of the evaporator, it existed as saturated vapor. The HPG was solely driven by steam, and there was no heat transfer from the system to the surroundings, except for the HPG, evaporator, condenser, and absorber. It is important to note that the exergy results did not include the exergy destruction of the burner in the boiler. Among the components of the multigenerational system, the combustion chamber exhibited the highest exergy destruction [13,14].

2.4. Operating Conditions

Table 2 presents the reference operating parameters that established the relationship between the system and its surrounding environment. The inlet and outlet temperatures of

steam, cooling water, and chilled water were regarded as external parameters, serving the purpose of maintaining energy balance within the respective system components.

Table 2. Operating parameters used in the simulation.

Component	Parameter	Values
HPG	T_{HPG} (°C)	193
	Inlet/outlet temperature of steam	T_{HPG} + 20/T_{HPG} + 5
MPG	T_{MPG} (°C)	134
LPG	T_{LPG} (°C)	66-82
Condenser	T_C (°C)	33
	Outlet/inlet temperature of coolant	T_C − 5/T_C − 10
Absorber	T_A (°C)	33
	Outlet/inlet temperature of coolant	T_A − 5/T_A − 10
Evaporator	T_E (°C)	5
	Outlet/inlet temperature of chilled water	T_E + 5/T_E + 10
	$\dot{Q}_E$ (kW)	100
Pump	η_P (%)	95
SHE I, SHE II, SHE III	$\varepsilon_{I,II,III}$ (%)	85

In single- to triple-effect absorption cooling systems, certain components, such as the evaporator, condenser, and absorber, are commonly present in each absorption cycle. The operational characteristics of these components have been extensively investigated in the literature. The evaporator temperature is constrained by two factors: the freezing point of water and the outlet temperature of chilled water. Typically, the evaporation temperature ranges between 4 °C and 10 °C. On the other hand, the condenser and absorber are responsible for heat rejection within the system. The outlet temperature of the condenser's cooling water is dependent on the operating temperature of the condenser, with a temperature difference of 5 K typically observed [1–3].

2.5. Biogas Content and Biogas Boiler

Biogas is a gaseous mixture composed of methane, carbon dioxide, nitrogen, oxygen, hydrogen sulfide, water vapor, ammonia, and low concentrations of hydrocarbons. The specific composition of biogas depends on the chemical characteristics of the biomass source and the method used for biogas production. It is important to note that, apart from methane, the other gases present in biogas are considered to be pollutants and are undesirable in the chemical composition of biogas [14]. The methane content in biogas typically ranges from 45% to 75% by volume, with the majority of the remaining gas being carbon dioxide. This variability in composition results in variations in the energy content of biogas. Different values for the lower heating value (LHV) of biogas are reported in the literature, reflecting these composition differences:

- 20,200 kJ/kg [12];
- 17,683 kJ/kg [7].

In this study, the biogas generated in the biogas digester, characterized by varying methane content, was directed towards a boiler. The heat generated through combustion served as the energy source to produce steam for the HPG. The boiler was equipped with a specific burner, exchanger, and other necessary components. Table 3 presents the methane compositions of the biogas utilized in the boiler while maintaining a constant percentage of H_2S (0.003%) and NH_3 (0.0001%) along with the corresponding lower heating values (LHVs).

Table 3. Methane composition of biogas used in boiler [20].

CH_4 (%)	~CO_2 (%)	LHV (kJ/kg)	LHV (kJ/m^3)
80	20	30,064.04	28,500.71
75	25	26,536.93	26,696.15
70	30	23,399.54	24,897.11
65	35	20,764.23	23,235.17
60	40	18,061.24	21,330.32
55	45	15,771.57	19,556.75
50	50	13,689.10	17,782.14
45	55	11,786.93	16,018.44
40	60	10,042.59	14,240.39

The heat provided by the fuel in the boiler was determined through the utilization of the equation presented as Equation (8) [25],

$$Q_{HPG} = Q_{boiler} = m_{fuel} * LHV_{fuel} * \eta_{boiler} \quad (8)$$

The equation incorporates the low calorific value of the biogas, denoted as LHV_{fuel}, which ranged from 10,042.59 kJ/kg to 30,064.04 kJ/kg. The overall efficiency of the boiler, denoted as η_{boiler}, was specified to be 80%.

The annual production of manure per animal is presented in Table 4. According to the table, individual cattle in the culture cattle category can produce 9125 kg of manure per year. When determining the potential biogas yield from animal wastes, it is important to consider the availability of manure and the dry matter content of the manure. In this study, the availability of manure was assumed to be 100% if a dedicated farm was established for each species. The solid waste rates for cattle, small ruminants, and poultry were taken to be 15%, 30%, and 35%, respectively. It was determined that 200 m^3 of biogas can be obtained from 1 ton of solid manure. The heating value of biogas was previously reported to be 22.7 MJ/m^3 in a reference study, but in this study, it was adopted as 23.2 MJ/m^3 with a 2% difference [26].

Table 4. Manure amount per animal species [27].

Species	Waste (kg/Year)	Species	Waste (kg/Year)
Domestic cattle	5475	Donkey	2737
Crossbred cattle	6570	Sheep	1095
Culture cattle	9125	Goat	730
Buffalo	7300	Hen (broiler)	27
Horse	5475	Laying hen	55
Mule	4380	Turkey	38
Pig	730	Goose	47
Camel	10,220	Duck	47

3. Results and Discussion

Figure 3 illustrates the increase in the COP of the system corresponding to biogas consumption and the component conditions. The COP value behaves as a single-effect system up to 67 °C, transitions to a double-effect system between 67 °C and 70 °C, and becomes suitable for a triple-effect system after 70 °C. At the end of the figure, the COP value reaches its maximum value of 1.78. As expected, the biogas consumption of the system decreases as the system's efficiency increases. Additionally, the biogas consumption of the system is influenced by the methane content. The minimum mass flow rate of biogas consumption is 0.0023 kgs^{-1} for an 80% methane content, while it is 0.0034 kgs^{-1} for a 65% methane content. This last result was utilized for estimating the required number of animals.

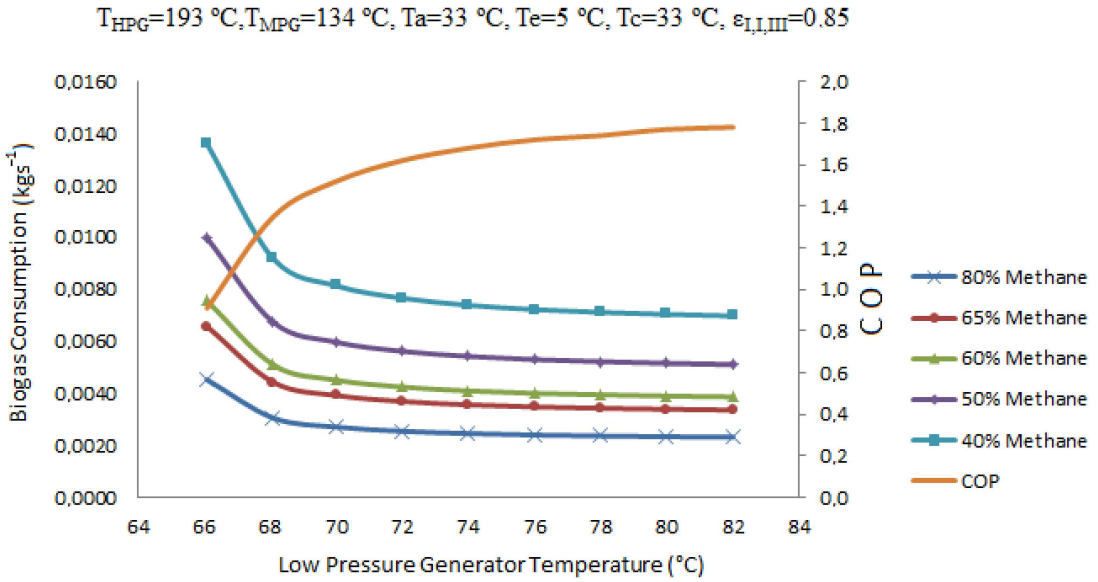

Figure 3. Variation in COP and biogas consumption of the system with LPG temperature.

Figure 4 presents the increase in the ECOP of the system as exergy destruction corresponding to the LPG and component temperatures varies. The high-pressure generator temperature and medium-pressure generator temperature are adequate to supply the necessary energy for internal thermal balance. The ECOP value demonstrates an increasing trend with higher LPG temperatures. At the end of the figure, the ECOP reaches its maximum value of 35.4%. The total exergy loss of the system exhibits a steep decrease at the beginning of the figure, gradually reducing until it reaches its minimum value of 57 kW at the end of the figure.

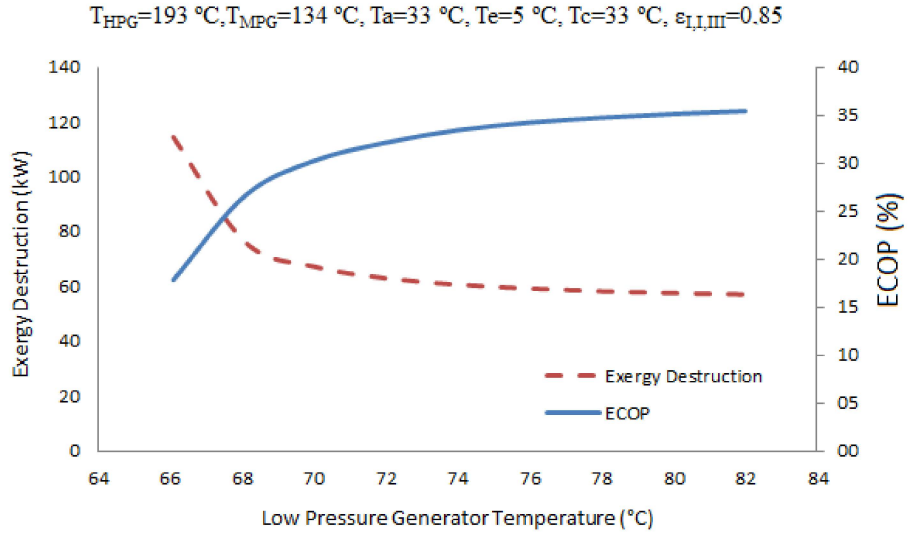

Figure 4. Variation in ECOP and exergy destruction of the system with LPG temperature.

Figure 5 illustrates the decrease in the COP of the system corresponding to biogas consumption and the component conditions. In the figure, the absorber and condenser temperatures increase together as equals. The minimum biogas consumption is at the beginning of the figure. The absorber and condenser temperatures cannot be less than 33°C because of the thermal unbalance in the system. Additionally, their temperatures cannot be more than 40°C because of the concentration of solution balance.

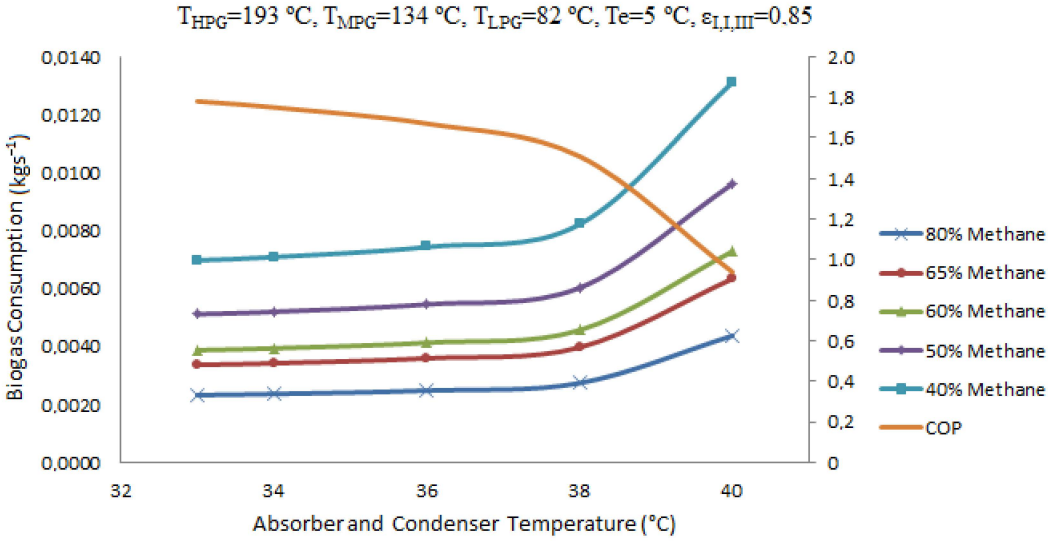

Figure 5. Variation in COP and biogas consumption of the system.

Figure 6 presents the decrease in the ECOP of the system. The absorber and condenser temperatures change together. The ECOP value demonstrates a decreasing trend with higher absorber and condenser temperatures. At the end of the figure, the ECOP reaches its minimum value of 18.6%. The total exergy loss of the system exhibits a steep increase at the end of the figure, gradually rising until it reaches its maximum value of 105.71 kW from its minimum value of 57 kW.

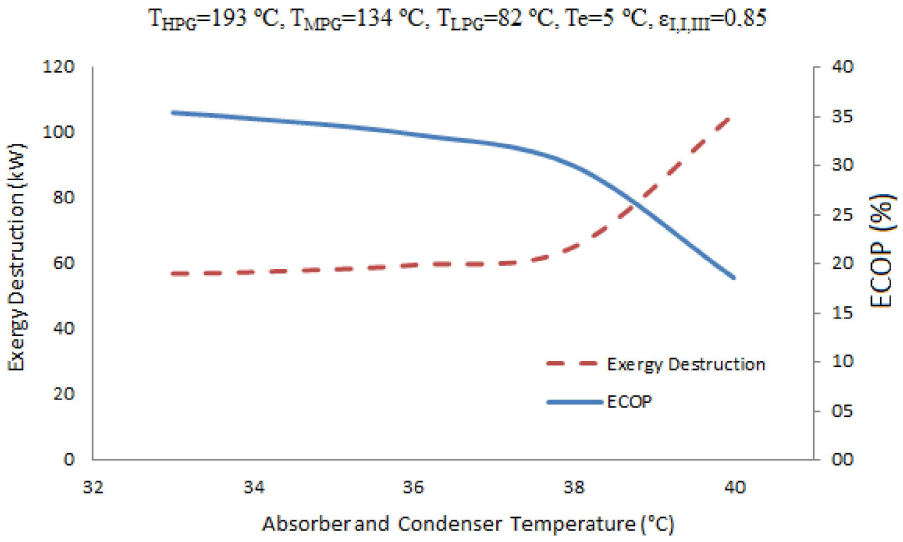

Figure 6. Variation in ECOP and exergy destruction of the system.

Table 5 provides the heat loads and exergy destruction of the different components of the system at their respective operating temperatures. The absorber exhibits the highest heat load, while the solution pump has the lowest heat load, which is negligible at 75 Watts and can be disregarded. These data are presented to facilitate the analysis of the exergy loss rates of the system components as depicted in Figure 7.

Table 5. Heat capacities and exergy destruction of the components.

T_{HPG} = 193 °C, T_{MPG} = 134 °C, T_{LPG} = 82 °C, $\varepsilon_{I,II,III}$ = 0.85, T_A = 33 °C, T_E = 5 °C, T_C = 33 °C		
Component	**Capacity (kW)**	**Exergy Destruction (kW)**
HPG	56.1	39.65
Absorber	117.6	6.66
Condenser	38.6	1.17
MPG	39.7	1.76
LPG	33.1	0.14
Evaporator	100	3.57
SHEs	94.8	2.56
Expansion valves	-	1.50

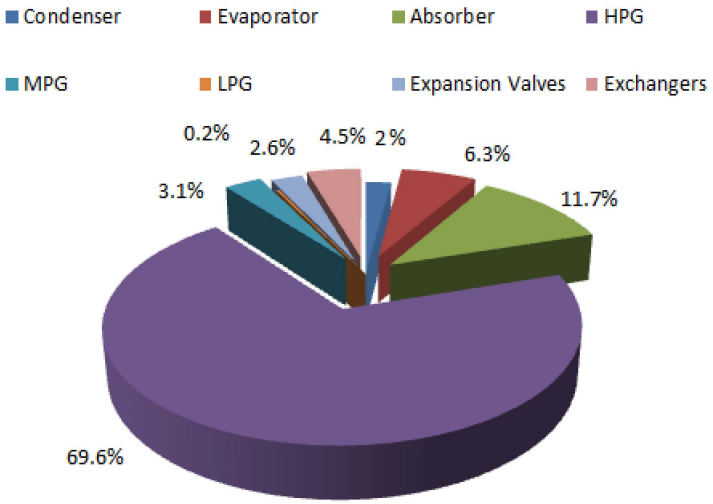

Figure 7. Exergy destruction rates of system components.

The overall exergy destruction represents the total exergy loss incurred by each individual component within the system. Each part of the system exhibits a specific exergy destruction rate. Figure 7 illustrates the exergy loss rates for each component. Under the specified conditions, the total exergy destruction amounts to 57 kW, with the highest contribution of 69.6% attributed to the HPG followed by the absorber with 11.7%. The exergy destruction in the pump is negligible and can be disregarded. The high exergy destruction in the HPG is primarily attributed to the steam exchanger side. In the case of the absorber, the main contributing factor is the highly inherent irreversible process involving the mixing of water vapor and the solution.

The final outcome of this study addresses the determination of the required number of animals for sixteen different species in a dedicated farm setting. Table 6 provides the calculated results, answering the fundamental question of "How many animals are necessary?" The answer is directly related to biogas consumption. As previously stated, for a methane content of 65%, the minimum flow rate of consumption is 0.0034 kgs^{-1}. Assuming the boiler operates for 20 h daily, the total annual consumption amounts to 88,721 kg. Considering that the density of biogas as 1.119 kg/m^3, the total volume of biogas required annually is 79,286 m^3. Since 200 m^3 of biogas can be obtained from 1 ton of solid animal waste, the annual solid waste requirement is calculated to be 396,431.1 kg.

Table 6. Sufficient number of animals per farm.

Species	Number	Species	Number
Domestic cattle	483	Donkey	966
Crossbred cattle	402	Sheep	1207
Culture cattle	290	Goat	1810
Buffalo	362	Hen (broiler)	41,954
Horse	483	Laying hen	20,596
Mule	603	Turkey	29,809
Pig	3621	Goose	24,101
Camel	259	Duck	24,101

The yearly manure production per animal was provided in Table 4 earlier, and the rates of solid waste for cattle, small ruminants, and poultry were also mentioned. The required number of animals varies for each species. Consequently, if a specialized farm is established for culture cattle, 290 cattle would be sufficient. However, a larger number would be necessary for the other two cattle species. For poultry species, a farm dedicated to laying hens would require 20,596 chickens to meet the requirements.

Consequently, the assessment of the cooling capacity in an animal production region can be conducted based on the necessary quantity of animals. In this study, the Bursa Province of Türkiye was selected to be the evaluated area. The geographical placement of Bursa within Turkey is depicted in Figure A1. Bursa is one of the crowded cities of Türkiye, and it is located in the Marmara Region. Bursa has seventeen districts and has a great amount of animal production. Table 7 gives the number of animals which are produced in Bursa [28]. There is no camel farming in the province. Furthermore, the population of pigs and mules is exceptionally scant. The other animal species are spread throughout the city. The availability of waste must be taken into account in determining the cooling potential from animal wastes. The availability of waste was selected to be 50% for cattle, 13% for small ruminants, and 99% for poultry. The number of biogas power plants that can be established according to biomass potential and availability are also given in Table 7.

Table 7. Number of livestock animals in Bursa.

Species	Animal Number	Potential Biogas Plant Number	Species	Animal Number	Potential Biogas Plant Number
Domestic cattle	8686	9	Donkey	1357	1
Crossbred cattle	60,816	76	Sheep	440,595	47
Culture cattle	164,721	284	Goat	82,603	6
Buffalo	2381	3	Hen (broiler)	4,694,577	111
Horse	3151	3	Laying hen	6,269,538	301
Mule	110	0	Turkey	55,386	2
Pig	90	0	Goose	6270	0
Camel	0	0	Duck	9166	0

As given in Table 7, the number of some animal species is not sufficient to feed 100 kW biogas-powered cooling loads individually. Small-scale biogas plants can be established in these livestock farms. Only cattle and chicken farms are suitable. Depending on the cultured cattle potential in Bursa, 284 biogas-powered cooling systems with a cooling load of 100 kW can be installed.

The livestock-derived biomass potential in Bursa is distributed across the entire city, which is divided into seventeen separate districts. Each district exhibits distinct animal production activities. While this study focuses on the biomass potential of the entire city, the need arises to assess each district individually. Furthermore, the considered cooling capacity may appear to be significant to many investors. Therefore, it is known that single-stage systems with smaller capacities are available in the market. Taking these factors into account, a new study has been initiated by the author to investigate the required animal

population for producing the necessary biogas to operate a single-stage absorption cooling system with a cooling capacity of 10 kW. The study aims to determine the feasibility of establishing such a facility in the Yenişehir District, which is known for its prominent livestock production in the Bursa Region.

4. Conclusions

This study focuses on conducting an efficiency evaluation of a biogas-operated cooling system through energy and exergy analyses. The cooling system, implemented in a rural area, utilizes a triple-effect absorption cycle. Initially, the minimum biogas consumption required to generate a fixed cooling capacity of 100 kW under various methane contents and operating conditions was determined. As a result, the minimum mass flow rate of biogas was found to be 0.0034 kgs^{-1} when the methane content was 65%, which is utilized to fuel the boiler. Based on this methane content, the required number of animals was calculated. Subsequently, the system's maximum COP and ECOP, along with the exergy loss of individual components, were determined under the same operating conditions. The highest COP recorded was 1.78, while the maximum ECOP reached 35.4% under the given operating conditions. Finally, to fulfill necessary biogas consumption, the study investigated the optimal number of animals for sixteen different species when establishing dedicated farms for each species. For instance, if a specialized farm is established for culture cattle, a total of 290 cattle would be deemed sufficient. In the case of poultry species, setting up a dedicated farm for laying hens would require 20,596 chickens to meet desired biogas consumption.

Funding: This research received no external funding.

Data Availability Statement: All data were mentioned in this paper. No external supporting data are available.

Conflicts of Interest: The authors declare no conflict of interest.

Nomenclature

COP	Coefficient of Performance
ECOP	Exergetic Coefficient of Performance
LPG	Low-Pressure Generator
MPG	Medium-Pressure Generator
MPC	Medium-Pressure Condenser
HPC	High-Pressure Condenser
HPG	High-Pressure Generator
H_2O	Water
LiBr	Lithium Bromide
NH_3	Ammonia
ORC	Organic Rankine Cycle
kWh	Kilowatt Hour
LHV	Lower Heating Value
SHE	Solution Heat Exchanger
CH_4	Methane
CO_2	Carbon dioxide
η	Efficiency
ε	Effectiveness

Appendix A. Maps of Türkiye

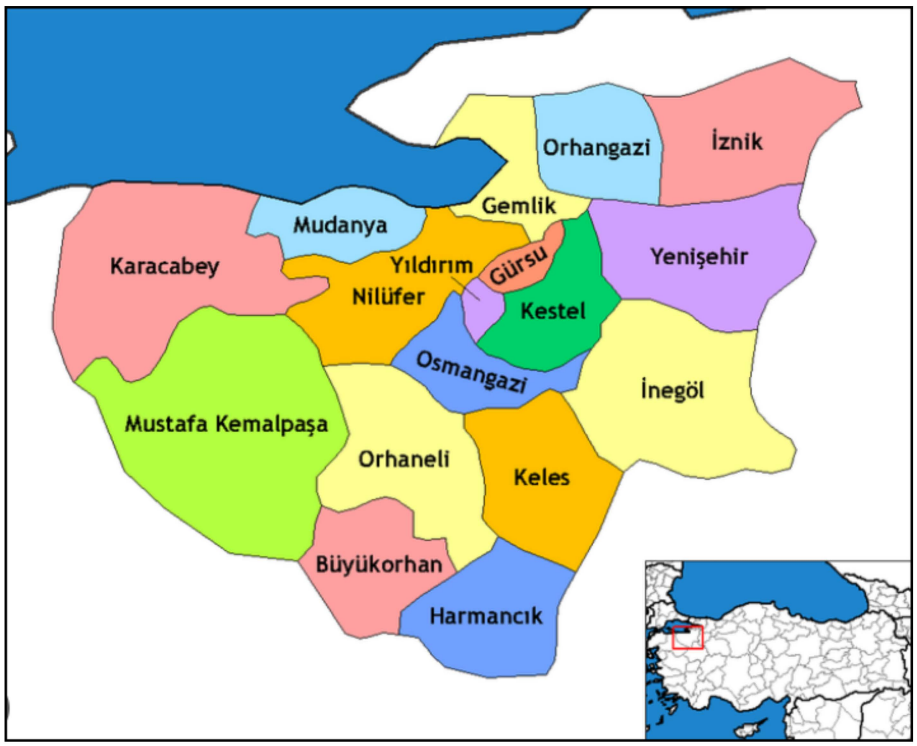

Figure A1. Location map of Bursa Province with districts in Türkiye.

References

1. Gomri, R. Investigation of the potential of application of single effect and multiple effect absorption cooling systems. *Energy Convers. Manag.* **2010**, *51*, 1629–1636. [CrossRef]
2. Saka, K. Evaluation of mass flowing with COP for triple effect absorption refrigeration system. *Bulg. Chem. Commun.* **2018**, *50*, 96–101.
3. Azhar, M.; Siddiqui, M.A. Optimization of operating temperatures in the gas operated single to triple effect vapour absorption refrigeration cycles. *Int. J. Refrig.* **2017**, *82*, 401–425. [CrossRef]
4. Azhar, M.; Siddiqui, M.A. Exergy analysis of single to triple effect lithium bromide-water vapour absorption cycles and optimization of the operating parameters. *Energy Convers. Manag.* **2019**, *180*, 1225–1246. [CrossRef]
5. Mahmoudi, S.M.S.; Salehi, S.; Yari, M. Three-objective optimization of a novel triple-effect absorption heat transformer combined with a water desalination system. *Energy Convers. Manag.* **2017**, *138*, 131–147. [CrossRef]
6. Gkouletsos, D.; Papadopoulos, A.I.; Seferlis, P.; Hassan, I. Systematic modeling under uncertainty of single, double and triple effect absorption refrigeration processes. *Energy* **2019**, *183*, 262–278. [CrossRef]
7. Ruwa, T.L.; Abbasoğlu, S.; Akün, E. Icle Energy and Exergy Analysis of Biogas-Powered Power Plant from Anaerobic Co-Digestion of Food and Animal Waste. *Processes* **2022**, *10*, 871. [CrossRef]
8. Velázquez, J.S.; Urueta, G.G.; Wong-Loya, J.A.; Molina-Rodea, R.; Franco, W.R.G. Cooling Potential for Single and Advanced Absorption Cooling Systems in a Geothermal Field in Mexico. *Processes* **2022**, *10*, 583. [CrossRef]
9. Lizarte, R.; Marcos, J.D. COP optimisation of a triple-effect H2O/LiBr absorption cycle under off-design conditions. *Appl. Therm. Eng.* **2016**, *99*, 195–205. [CrossRef]
10. Gebreslassie, B.H.; Medrano, M.; Boer, D. Exergy analysis of multi-effect water–LiBr absorption systems: From half to triple effect. *Renew. Energy* **2010**, *35*, 1773–1782. [CrossRef]
11. Agarwal, S.; Arora, A.; Arora, B.B. Energy and exergy analysis of vapor compression–triple effect absorption cascade refrigeration system. *Eng. Sci. Technol. Int. J.* **2020**, *23*, 625–641. [CrossRef]
12. Schneider, J.V.; Malmquist, A.; Araoz, J.; Herrero, J.M.; Martin, A. Performance Analysis of a Small-Scale Biogas-Based Tri-generation Plant: An Absorption Refrigeration System Integrated to an Externally Fired Microturbine. *Energies* **2019**, *12*, 3830. [CrossRef]
13. Bamisile, O.; Huang, Q.; Anane, P.O.K.; Dagbasi, M. Performance Analyses of a Renewable Energy Powered System for Trigeneration. *Sustainability* **2019**, *11*, 6006. [CrossRef]
14. Sevinchan, E.; Dincer, I.; Lang, H. Energy and exergy analyses of a biogas driven multigenerational system. *Energy* **2019**, *166*, 715–723. [CrossRef]

15. Anand, S.; Gubta, A.; Tyagi, S.K. Critical analysis of a biogas powered absorption system for climate change mitigation. *Clean Techn. Environ. Policy* **2014**, *16*, 569–578. [CrossRef]
16. Maryami, R.; Dehghan, A.A. An exergy based comparative study between LiBr/water absorption refrigeration systems from half effect to triple effect. *Appl. Therm. Eng.* **2017**, *124*, 103–123. [CrossRef]
17. Kaynakli, O.; Saka, K.; Kaynakli, F. Energy and exergy analysis of a double effect absorption refrigeration system based on different heat sources. *Energy Convers. Manag.* **2015**, *106*, 21–30. [CrossRef]
18. Yılmaz, İ.; Saka, K.; Kaynakli, O. A thermodynamic evaluation on high pressure condenser of double effect absorption refrigeration system. *Energy* **2016**, *113*, 1031–1041. [CrossRef]
19. Yılmaz, İ.; Saka, K.; Kaynakli, O.; Kaşka, Ö. Performance Assessment and Solution Procedure for Series Flow Double-Effect Absorption Refrigeration Systems Under Critical Operating Constraints. *Arab. J. Sci. Eng.* **2019**, *44*, 5997–6011. [CrossRef]
20. Caetano, B.C.; Santos, N.D.S.A.; Hanriot, V.M.; Sandoval, O.R.; Huebner, R. Energy conversion of biogas from livestock manure to electricity energy using a Stirling engine. *Energy Convers. Manag. X* **2022**, *15*, 100224. [CrossRef]
21. Yılmaz, İ.; Saka, K. Exploitable biomass status and potential of the Southeastern Anatolia Region, Turkey. *Energy Sources B Econ. Plan. Policy* **2018**, *13*, 46–52. [CrossRef]
22. Available online: https://www.thermaxglobal.com/tripple-effect-chiller/ (accessed on 18 May 2023).
23. Gomri, R. Thermodynamic evaluation of triple effect absorption chiller. In Proceedings of the 2008 Second International Conference on Thermal Issues in Emerging Technologies, Cairo, Egypt, 17–20 December 2008.
24. Küçük, E.Ö.; Kılıç, M. Exergoeconomic and Exergetic Sustainability Analysis of a Combined Dual-Pressure Organic Rankine Cycle and Vapor Compression Refrigeration Cycle. *Sustainability* **2023**, *15*, 6987. [CrossRef]
25. Köse, Ö.; Koç, Y.; Yağlı, H. Performance improvement of the bottoming steam Rankine cycle (SRC) and organic Rankine cycle (ORC) systems for a triple combined system using gas turbine (GT) as topping cycle. *Energy Convers. Manag.* **2020**, *211*, 112745. [CrossRef]
26. Avcioğlu, A.O.; Türker, U. Status and potential of biogas energy from animal wastes in Turkey. *Renew. Sustain. Energy Rev.* **2012**, *16*, 1557–1561. [CrossRef]
27. Saka, K.; Yılmaz, İ.H.; Canbolat, A.S.; Kaynaklı, Ö. Energy potential of animal biomass in Turkey. *Eur. J. Tech.* **2018**, *8*, 160–167. [CrossRef]
28. Available online: https://bepa.enerji.gov.tr/ (accessed on 18 May 2023).